Journal of Petroleum Exploration and Production Technology (2020) 10:3007–3023
https://doi.org/10.1007/s13202-020-00893-6

ORIGINAL PAPER-PRODUCTION ENGINEERING

Numerical and experimental study on a bypass pig motion in oil transmission pipeline: a case study

Asghar Talbizadeh[1] · **Mohammad Mehdi Keshtkar**[1]

Received: 25 February 2020 / Accepted: 18 April 2020 / Published online: 30 April 2020

Abstract

In the oil and gas industry, pipeline networks can be used to transport oil and petroleum products from production center to the consumption center. Regular cleaning and inspecting these pipelines is necessary due to the presence of oil deposits. Typically, pigging operation can be applied to clean and inspect of these pipelines. It is important that the velocity of a pig during its passage in the oil pipeline be controlled. Therefore, it is necessary to identify accurately the fluid flow around the pig in order to describe and evaluate the pigs' motion. In this study, the computational fluid dynamics (CFD) approach has been applied to model fully turbulent flow around a sample of bypass pig and measure its dynamic velocity. This study tried not only to study the pig motion, but also to investigate the parameters affecting the bypass pig pressure drop and then the optimal state of these basic parameters in the design of a pig is determined. Finally, a numerical analysis of the pig motion is performed for a case study of a 20-ih pipeline to transport of gas oil between Rafsanjan, Yazd and Nain located in Iran and compared with the field test results. The results indicated that the fluid passing through the bypass, the weight and contact force had a significant effect on the pig's speed, and when bypass diameter was larger, leading to the greater fluctuations.

Keywords Transmission pipeline · Hydrodynamic optimization · Pig · Bypass · Computational fluid dynamics

List of symbols

D (m)	Pipe diameter
d (m)	Diameter in the bypass hole of pig
H (m)	Disk height
$h(m)$	Disk height
$K_p(-)$	Pressure loss coefficient
L (m)	Length
P (Pa)	Pressure
P_t (Pa)	Total pressure
t (m)	Disk Thickness
u (m/s)	Velocity
V (m/s)	Average velocity
y (m)	Distance from the pipe wall

Greek symbols

μ (kg/ms)	Dynamic viscosity
ν (m^2/s)	Kinematic viscosity
ρ (kg/m^3)	Density
τ (Pa)	Shear stress of wall

✉ Mohammad Mehdi Keshtkar
Mkeshtkar54@yahoo.com

[1] Department of Mechanical Engineering, Kerman Branch, Islamic Azad University, Kerman, Iran

Introduction

The speed control of the pig can be considered as one of the important problems for the pigging operation due to the limitation in speed and fluid flow inside the pipe. Lack of ability to control the speed of the pig can be caused both no cleaning, and in some more sensitive situations, collecting no information by means of the sensors installed on the pig. There are several methods of speed control of the pig and one of them is the use of bypass to control the pressure difference between the front and back of the pig. The estimation and control speed of pig and the time pig reaches the end of pipelines can greatly help the pipeline pigging success. Several researchers have studied the flow around the bypass pigs. McDonald and Baker (1964) were probably the first investigators to present a study on pigging operation and obtained the equation of motion of the pig. It has been argued that pigging of pipeline can increase the fluid transfer efficiency from 30 to 70%. Kohda et al. (1988) developed first pigging simulation model based on full two-phase transient flow formulation. The results were summarized using both the finite-difference numerical method and two fixed and moving coordinate systems. Numerical solution and experimental results agree very well. Azevedo et al. (1996) examined pig motion through horizontal pipelines,

and single-phase fluid flow was assumed to be incompressible and steady state. Moreover, the hydrodynamic model of the bypass flow passing through the pig was analyzed and simplified. Singh and Henkes (2012) investigated the simple bypass pig model for static two-phase flow using ANSYS-FLUENT software. They calculated the pressure drop coefficient for a given bypass diameter in high Reynolds numbers and showed that the results obtained from numerical simulation were consistent with the theoretical relations in Ref. Idelchik (1987).

Braga et al. (1998) investigated simulation of the bypass pig motion in gas and liquid pipelines. The equations expressing mass, momentum and state conservation laws for an incompressible fluid flow within a pipeline were considered and combined with equations expressing the pig equilibrium and the bypass flow that passed through the pig body. The results obtained from this study were shown for three states of the pig motion within a pipeline: (1) the pig motion for dehydrating or drying, (2) the pig motion in gas pipelines, and (3) the pig motion in pipelines despite the bypass flow. Nguyen et al. (2001) studied the dynamical analysis of the pig motion through the straight horizontal gas pipelines. They analyzed ideal gas, single-phase one-dimensional fluid flow, a horizontal constant-diameter pipe, the coefficient of friction was found to be a function of the Reynolds number, the roughness of the pipe wall and compressible non-uniform gas flow. This study analyzed dynamic behavior characteristics such as gas fluid flow, the pig position and velocity. This reference achieved the pig suitable speed for the pigging operation for pipes with a compressible fluid of 1 to 5 m/s and for pipes with an incompressible fluid of 2 to 7 m/s. A numerical simulation of pig motion with bypass flow through gas pipelines was presented by Hosseinalipour et al. (2007). Similar to the Ref. Braga et al. (1998), equations expressing continuity, linear momentum and state for compressible gas flow were considered and then these equations together with the pig and bypass flow equations were solved using finite difference method by staggered lattice. Gas was modeled as both ideal and real. By comparing these results, it was found that the dynamic behavior of the pig in both cases was similar and did not differ significantly. Therefore, given the large increase in the volume of calculations for the real gas model, the ideal gas assumption was useful and cost-effective. Esmaeilzadeh et al. (2009) developed mathematical modeling and simulation of pigging operation in gas and liquid pipelines. In this study, the gas flow was assumed to be single-phase, one-dimensional, and non-isothermal, but fluid flow was found to be single-phase and isothermal in straight pipelines. The simulation of pig motion in gas and liquid pipelines was studied for flow rates of various fluids, and in each case the pig velocity curve was plotted. For the first time, Saeedbakhsh et al. (2009) studied dynamic modeling of small pig in space pipeline. In this research, the effect of the flow field on the pig motion was ignored and only the driving force was assumed to be time-dependent, but the coefficient of friction was assumed to be constant and pig was small for the sake of simplicity. The obtained equations were evaluated for three pipe samples. Lesani et al. (2012) used the equations of Ref. Saeedbakhsh et al. (2009) and combined them with equations expressing compressible fluid flow and the bypass flow and then performed the dynamic analysis of the pig with a bypass flow through the two and three dimensional liquid pipelines. Simplistic assumptions such as being constant the pig/wall friction coefficient and incompressible fluid have been used to extract equations. In this study, the fluid velocity was also considered to be constant. Davodian (2014) performed simulation of pig motion in gas and liquid pipelines. In this research, fluid flow was assumed to be single-phase and one-dimensional and the cross-sectional area of the pipe was assumed to be constant in straight pipelines. Korban (2014) studied the flow around the pig in a static state. A two-dimensional axisymmetric model was applied to investigate the fluid flow around two types of bypass pigs used in the oil and gas industry, namely ordinary pig and the disk pig. A careful behavior of flow around of a bypass pig was also investigated. In addition, various parameters were studied to investigate the relationship between the total pressure loss coefficient and the governing parameters on the bypass pig. Ramirez and Dutra (2011) used pig models with different bypasses to minimize the force acting on the constant pig by fluid and also maximize the pig size for the placement of devices such as a battery, electric boards and so on. It has been argued that if bypass had the same inlet and outlet diameters, dramatic changes in flow would occur in front and back of pig, and to prevent this phenomenon, three types' profiles of conical pig and nozzle pig were used and the force acting on the pig by fluid is obtained for all three profiles. Nshuti (2016) studied the flow around pig in dynamic mode using the ANSYS LS-DYNA software.

The purpose of this study is to investigate the effect of bypass diameter on the fluid flow behavior while pig passes through pipeline, and examine its speed and motion in gas oil pipeline between Rafsanjan, Yazd and Nain in Iran as a case study. In the present study, a careful behavior of the flow around the bypass pig is considered. The effect of bypass diameter, pre-deflector plate size and the distance between the plate and the bypass hole is investigated, and then the optimal design of the bypass pig in order to have the best efficiency of cleaning the internal pipe wall surface with the lowest possible pressure drop, pig velocity in dynamic mode is determined while moving through the pipeline.

Theory

Problem statement

Figure 1 shows a two-dimensional presentation of a horizontal pipe with diameter D and a bypass pig inside it. Gray plates indicate the pig and the pig wall is in contact with the internal pipe wall surface. A single-phase and viscous Newtonian fluid enters the pipe with mass flow rate $\dot{m}$. Incompressible, steady and turbulent flow is assumed. In the distance h from bypass outlet, the disk deflector plate with diameter H has a thickness t that blocks the flow, so the flow has to pass around this plate. The flow from the left side of the pipe strikes the disk and passes through the bypass passage with diameter d. In this study, the effect of change in 1 to 8 in bypass diameter on the pig velocity along the route of the pipeline of gas oil is studied. At the inlet site, the average flow rate is 850 kg/h. Other input values of the problem are listed in Table 1:

Considering a 0.5 in relative step, the bypass diameter increased from 1 to 8 in during 15 steps, and each increased step, the average speed of the pig was calculated at each level. The path of the pig motion has been shown in Appendix 1. The beginning of the pipeline pig is in Rafsanjan's pump room with an altitude of 1453 m above sea level. The gas oil with a flow rate of 850 kg/h from the altitude would be sent to the Yazd Oil Transportation center in 224 km. The Yazd Oil Transportation center is located at an altitude of 803 m above sea level. This center carried out again transportation operation of petroleum product via pumping during a 234 km path to the Nain Oil Transportation Center at 1759 height. According to this map, the length of the path can be divided into 34 cross sections with respect to the lines included within profile based on the slope of the pipeline and its continuity (Appendix 2).

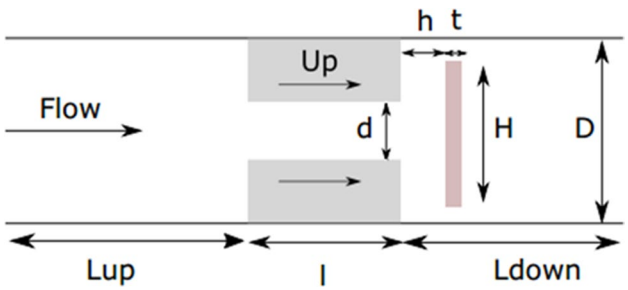

Fig. 1 The two-dimensional presentation of the bypass pig in the pipe

Table 2 shows the diameter of the selected bypasses for a disk pig in the 20-in pipeline between Rafsanjan, Yazd and Nain with other geometrical specifications.

In each cross section, due to the slope of the pipeline and its height, the static pressure is calculated and considered as the initial condition of the software. Static pressure at the beginning and end of the cross sections on the map of the pipeline profile is extracted. The pipeline outlet pressure at the Yazd Transmission Center at 225 km is equal to 150 psi, and the pipeline outlet pressure at the Nain Oil Transmission Center at the end of the pipeline is 50 psi based on the calculated utilization data. It should be noted that both the weight and prevention of formation sediments in the front of the pig for the simulation are ignored.

Governing equations

If density, velocity, pressure and area with the parameters ρ, v, P and A are taken into account and gravitational acceleration symbolized g, the stress resulting from the viscosity force acting on wall be is τ, with considering Fig. 2 and writing mass and momentum conservation laws, the governing equations can be expressed as follows:

$$\frac{\partial(\rho AV)}{\partial t} + \frac{\partial(\rho AV)}{\partial x} = 0 \tag{1}$$

Table 2 Selected bypass diameter for disk pig in 20-in pipeline between Rafsanjan, Yazd and Nain

$d\,(in)$	$d\,(cm)$	$\left(d^2/H^2\right)(\%)$	$A_d\,(m^2)$
1	2.54	0.25	0.000506
1.5	3.81	0.56	0.001139
2	5.08	1	0.002025
2.5	6.35	1.56	0.003165
3	7.62	2.25	0.004558
3.5	8.89	3.06	0.006204
4	10.16	4	0.008103
4.5	11.43	5.06	0.102556
5	12.7	6.25	0.012661
5.5	13.97	7.56	0.015320
6	15.24	9	0.018232
6.5	16.51	10.56	0.021397
7	17.78	12.25	0.024816
7.5	19.05	14.06	0.028487
8	20.32	16	0.032412

Table 1 Problem input data

$D\,(in)$	$h\,(in)$	$H\,(in)$	$m\,(kg)$	$d\,(in)$	$\dot{m}\,(kg/hr)$	$T_{in}\,(^\circ C)$	$\mu\,(\mathrm{kg/ms})$	$\rho\,(kg/m^3)$	*Fluid*
20	1	4	15	2	850	55	0.00332	829	Gas–Oil

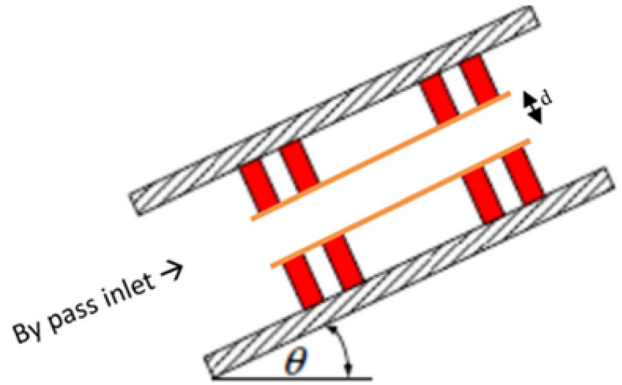

Fig. 2 A schematic of the bypass pig in slope steep pipeline

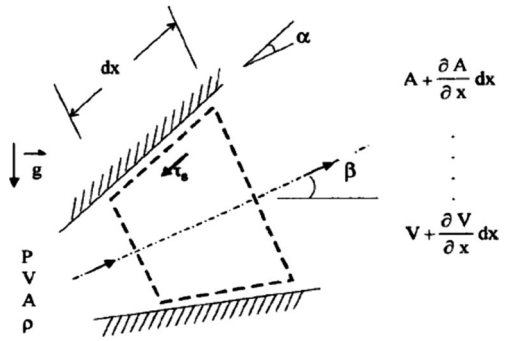

Fig. 3 The control volume for a pig motion in pipe line at the steady state condition

According to the control volume considered in Fig. 3, the momentum equation is achieved as follows:

$$\rho\frac{DV}{Dt} = -\frac{\partial p}{\partial x} - \frac{\tau_s P_m \mathrm{Cos}\,\alpha}{A} - \rho g \ \sin\ \beta \tag{2}$$

If the f is considered as the coefficient of dynamic friction caused by the viscosity force and the assumption of $\mathrm{Cos}\,\alpha \simeq 1$, the momentum equation is summarized as follows:

$$\frac{\partial V}{\partial t} + V\frac{\partial V}{\partial x} = -\frac{1}{\rho}\frac{\partial p}{\partial x} - \frac{f}{2}\frac{|V|\,V}{D} - g\,\mathrm{Sin}\,\beta \tag{3}$$

The friction coefficient f depends on the Reynolds number and also in turbulent flow to the roughness coefficient of the pipe surface. The friction coefficient is examined by assuming that the flow is fully developed. Therefore, for turbulent flow the friction coefficient is calculated using the relationship of Miller as follows:

$$f = 0.25\left\{\log\left[\frac{\varepsilon/D}{3.7} + \frac{5.74}{\mathrm{Re}^{0.9}}\right]\right\}^{-2} \tag{4}$$

The Paige movement with fluid flow in the pipe will reach a force balance and a pressure loss is caused by passing the flow through the bypass of Paige. The equation of this balance is achieved according to Eq. (2).

The pig motion with the fluid flow in the pipeline is obtained through a force balance as follows. This equation is based on the calculation of the forces acting on pig in the present study:

$$m\frac{\mathrm{d}V_{\mathrm{pig}}}{\mathrm{d}t} = (P_1 - P_2)A - mg\ \sin\theta - F_c \tag{5}$$

where V and m are the velocity and mass of the pig, respectively, p_1 and p_2 denote the pressure at each side of the pig and F_c is the axial contact force acting on pig with the inside surface of the pipe known as the contact force. This force depends on both the position of a pig along the pipeline and the pig velocity. When the pig remains constant inside the pipe, the contact force is zero. When the pig moves through the fluid, the contact force is assumed to be constant expressing F_{dyn} as dynamical friction. Depending on the direction of the motion of the pig, this force is defined as follows:

$$F_c = \begin{cases} -F_{\mathrm{dyn}}(x_{\mathrm{pig}}) & \text{if } V_{\mathrm{pig}} < 0 \\ F_{\mathrm{dyn}}(x_{\mathrm{pig}}) & \text{if } V_{\mathrm{pig}} > 0 \end{cases} \tag{6}$$

The equations have been presented so far are respective to the pig does not have a bypass. According to Fig. 2, a bypass with diameter d is now considered. With considering the mass conservation law, the volume of fluid at the bypass hole can be calculated by the following equation:

$$Q_h = Q - V_{pig}A \tag{7}$$

where Q_h is the volume rate of the fluid at the bypass hole,Q is the volume of the fluid at the upper part of the pig (pig's back) and A is the cross-sectional area of a pipe. The pressure drop on both sides of the pig can be written as Eq. (8) according to the relationship between the fluid at the side path of the pig and pressure difference at its two sides, where K_p denotes the localized pressure drop coefficient and V_d is the velocity of the fluid velocity at the bypass hole:

$$P_1 - P_2 = K_p\rho\frac{V_d^2}{2} \tag{8}$$

Finally, equation expressing mass conservation for the desired control volume can be written as follows:

$$P_1 - P_2 = \frac{K_p\rho}{2}\left[\left(\frac{A}{A_d}\right)^2\left(\frac{Q}{A} - V_{\mathrm{pig}}\right)^2\right] \tag{9}$$

where A_d is the area of the bypass hole and V_{pig} is the average pig velocity. The pressure loss coefficient, K_p, for the disk bypass pig can be calculated by Ref. Idelchik (1987) for a thick hole. Figure 4 illustrates the two-dimensional schematic of the flow around a disk pig. In fact, the considered pig is a combination of a sudden contraction in the face of a flow deflector plate.

Using both geometry in the present study and Eq. (10), the pressure loss coefficient can be calculated for the desired bypass pig.

$$K_p \approx 0.5\left(1-\frac{F_0}{F_1}\right)^{0.75}+\left(1-\frac{F_0}{F_1}\right)^{2} \tag{10}$$

In addition, in this study to optimize the pig performance in the pipeline, a list of dimensionless groups is considered as follows:

- Dimensionless group $\left(\frac{d}{D}\right)^2$ which represents the ratio of the cross-sectional area of the bypass to the cross-sectional area of a pipe. This non-dimensional parameter shows the degree of contraction of fluid at the bypass pig.
- Dimensionless group $\left(\frac{H}{D}\right)$ which indicates the ratio of the diameter of the deflector plate to the diameter of the pipe.
- Dimensionless group $\left(\frac{4dh}{D^2}\right)$ which represents proportion of the smallest level of fluid emerging between the deflector plate and the disk to the disk surface of the pig.

The specified parameters are used to optimize the dimensions of the pig for the purpose of the pig performance in future sections.

Simulation Technique and Problem-solving Process

In this study, all simulation operations to solve of problem were performed using commercial package ANSYS FLUENT18. After considering the geometry for desired problem, the data for fluid flow, bypass pig and the boundary conditions of the numerical model were first determined. Then, using the required settings in the software, the mesh strategy was carefully examined and finally, the user defined function (UDF) was applied to implement dynamically the pig motion. Since the ANSYS FLUENT software cannot independently consider dynamically the motion of an object and does not have a direct simulation capability, one of the most important numerical simulation challenges of this software is the provision of UDF to specify the dynamic equations and the new position of the pig to the software. To create this movement in transient flow, an UDF program has been written in Visual Studio V.11 to calculate both force acting on pig and a new position. The UDF calculates the forces acting on the pig at any moment, and the position of the pig will be changed in accordance with the obtained forces. This process is performed at any time step, and then this loop is repeated to calculate the forces and, consequently, the new position created at a later time step. UDF algorithm has been shown in Fig. 5.

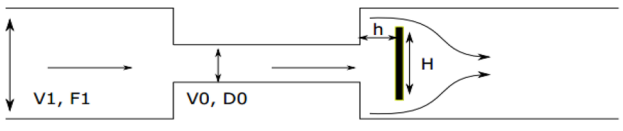

Fig. 4 Initial design of flow around a disk pig to calculate the pressure drop at the two sides of the pig (Ref. (Idelchik 1987))

Results and discussion

In order to control the pig velocity in pipeline between Rafsanjan,Yazd and Nain as a case study in Iran, the desired problem as numerically is simulated hydrodynamically. According to the path map, the length of the path with respect to the pipelines included within profile based on the slope of the pipeline and its continuity is divided into 34 cross sections, which the results of this analysis are presented in the following section:

Validation

In order to check the accuracy of the problem solution in the transient state, the simulated model has been compared with the results presented in the Ref. (Nguyen et al. 2001). As shown in Fig. 6, the form of the considered reference problem included a pipe and the path coordinates, has been presented in Table 3, which is used to discharge water inside its path by a pig with nitrogen gas. The length of the path is 1500 m and the pipe diameter is 10 ins. The weight of the pig for liquid discharge of this path is 3 kg, the contact force is ± 4982 N, which this value of force is considered to create a pressure of the cross-sectional area of the pig. At first, the liquid is located constant in the pipeline before moving the pig, and there is a hydrostatic pressure distribution by means of it. During the discharge process, the outlet pressure is held constant on 10 atm. The flow rate of consumption gas of the pig's back is varied linearly from zero to 3 kg/s for 10 s. After that, this flow rate is held constant and also at the starting point, the pig has a speed of zero.

In this study, the result of simulating the position and velocity of the pig along the path and the results obtained from Ref. (Nguyen et al. 2001) are shown in Figs. 7 and 8, respectively.

As can be seen from Fig. 7, as long as the outlet pressure is constant, the inlet pressure extends an increased trend during time to reach point 3 (approximately 820 s).

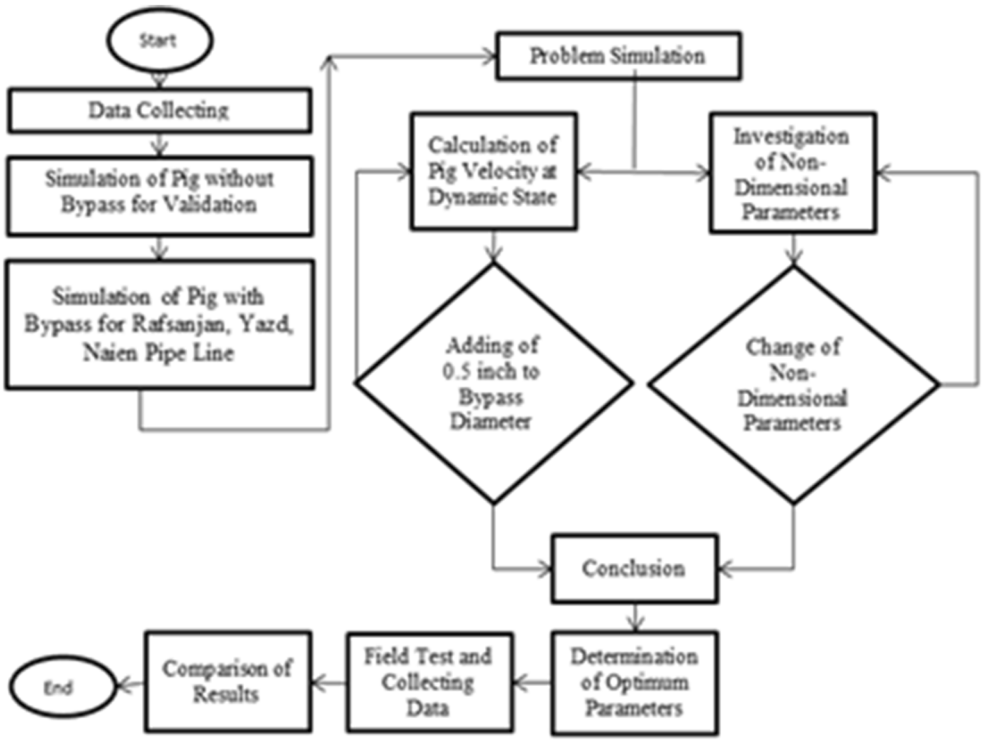

(a)

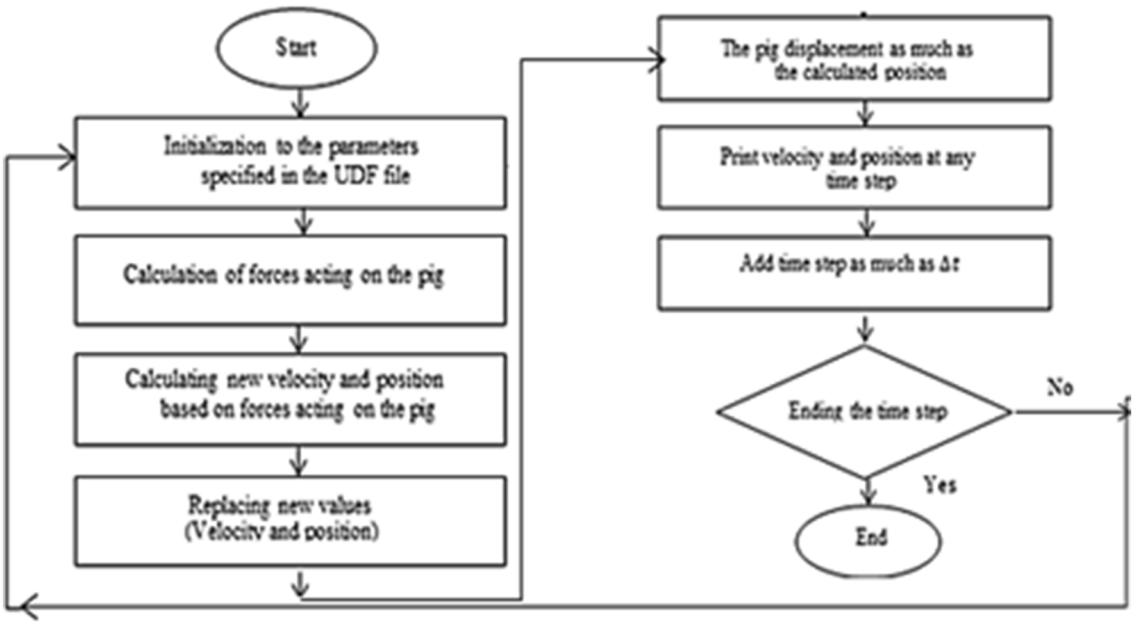

(b)

Fig. 5 **a** Problem-solving algorithm, **b** UDF algorithm

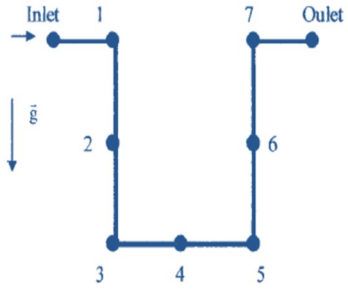

Fig. 6 A schematic of the U-shaped pipeline in Ref. (Nguyen et al. 2001)

This behavior caused by as the pig moves downward with respect to the direction of the pipe at this cross section. When the pig moves from point 3 to point 5 (the time between 820 and 1080 s), the inlet pressure is almost constant because the pressure of the water column after the pig is constant at this cross section and then the inlet pressure decreases due to the reduction of the water column in front of the pig.

Figure 8 illustrates the velocity diagram as a function of the pig position. Comparison between Figs. 8a, b in addition to the proper fit shows that the pig initially takes a significant velocity to reach point 1 due to the existence of a small hydrostatic pressure. As the pig moves downward, the velocity decreases by increasing the hydrostatic column of the water. The velocity of the pig remains almost constant in the vertical parts of the path, and when it reaches the end of the vertical part or the point 3, the pig velocity increases sharply due to the decrease in the resistance of the liquid column.

Results

To check the mesh independency, three different sizes of mesh have been created and problem simulated according to these models. Consistency must be reduced to an acceptable value and solution demonstrates convergence. At first, the primary mesh of 1,901,856 cells is constructed, and the drag coefficient of the pig is calculated. Then, a secondary mesh, whose size is usually 1.5 times the previous mesh,

Table 3 The coordinates of the points of the U-shaped pipeline of Fig. 6

Position	X (m)	y (m)	L (m)	Position	x (m)	y (m)	L (m)
Inlet	0	0	0	5	250	-600	850
1	50	0	50	6	250	-300	1150
2	50	−300	350	7	250	0	1450
3	50	−600	650	Outlet	300	0	1500
4	150	−600	750	–	–	–	–

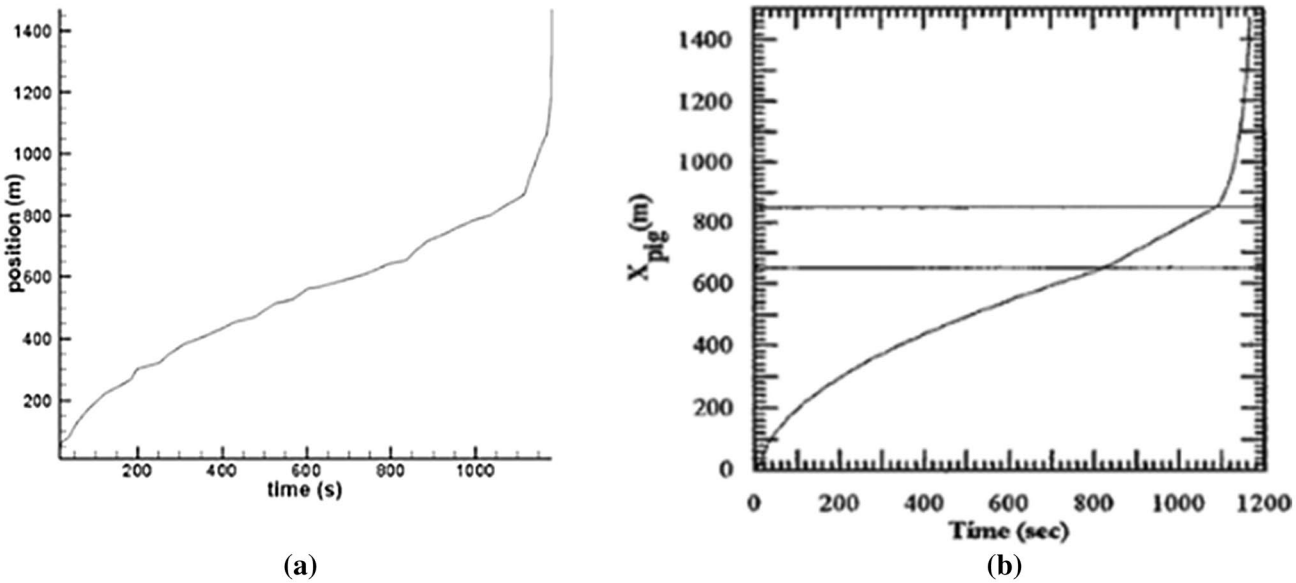

Fig. 7 The simulation results related to the changes in pig position relative to time **a** in the present study **b** numerical results of Ref. (Nguyen et al. 2001)

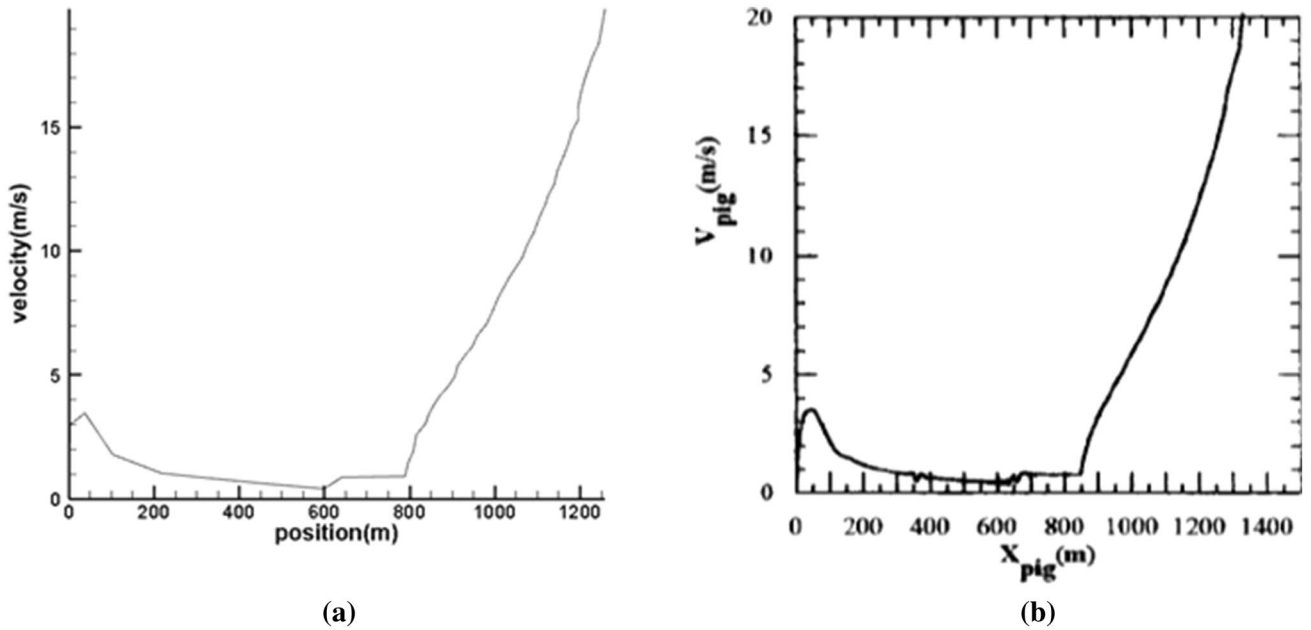

Fig. 8 Change in pig velocity relative to position **a** in the present study **b** numerical results of Ref. (Nguyen et al. 2001)

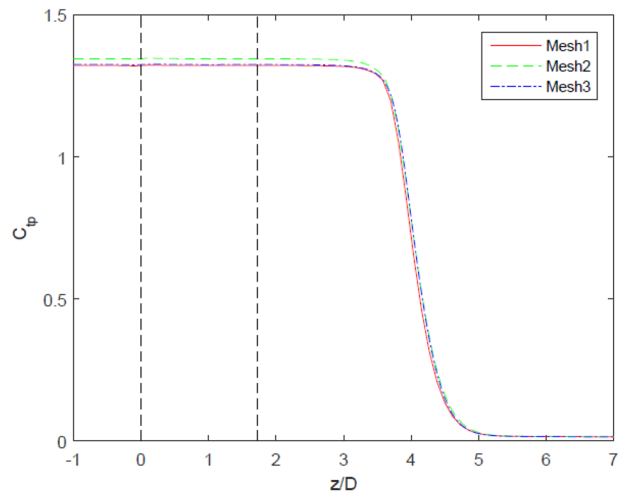

Fig. 9 Checking the mesh independency for simulation

is constructed (4,044,663 cells). The results from the two different meshes are compared. If the results were unacceptable, the third mesh is required by further processing. The third mesh of 9,511,515 cells is tested for flow analysis at bypass. The results of mesh independency have been shown in Fig. 9.

After checking the mesh independency and considering the secondary mesh with 4,044,663 cells, simulation of the desired problem is performed. After examining the results obtained by the software, there are two different behaviors around a disk pig with a deflector plate. The streamlines and pressure contour for these two different behaviors of the flow around a disk pig have been shown in Fig. 10. As shown in Figs. 10a–f, two different behaviors are created by changing in the dimensionless parameters as follows:

Behavior A: In this type of flow behavior in the bypass area of disk, a jet is formed. After the jet leaves bypass area of disk, it first strikes the deflector plate and then, the jet moves along the disk and the pipe wall downward. An area with a rotating flow is created between the jet and the disk pig. At the bottom of the pipe, the main rotating area which is below the jet strikes the pipe wall.

Behavior B: In this behavior, the jet does not strike the disk pig but is directly in contact with the bottom wall of the pipe. Therefore, the area with the rotating flow is located between the pig body and the jet at the center of the pig wall and the bottom wall of the pipe. The main rotating area is still at the center of the bottom pipe.

Figures 10c, d show the pressure drop around the bypass pig under study. These figures show that the total pressure drop will be increased by changing in the flow behavior from A to B. It is also shown that the total pressure drop occurs mainly in the area after the deflector plate. For behavior A, the minimum total pressure is located in the rotating area between the jet and the deflector plate while there is a minimum total pressure in the rotating area between the center and pipe wall for the behavior B. By analyzing the flow velocity of Figs. 10e, f, in both behavior, the maximum velocity occurs when the jet strikes the top of the deflector plate. In the upstream and downstream of pipe, the flow moves at its moderate velocity, but in the rotating area in the

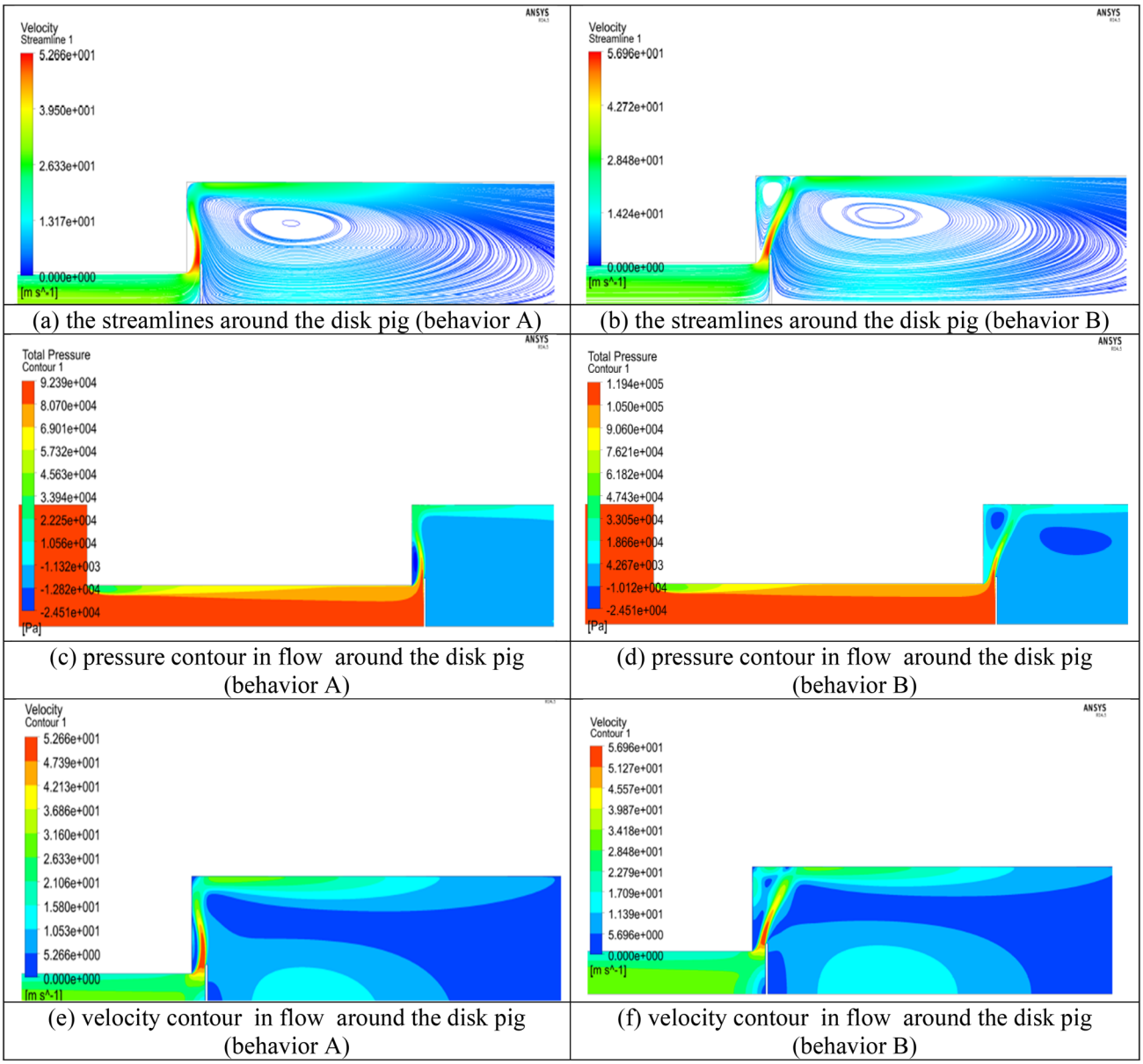

Fig. 10 The flow pipelines and pressure contour for two different behavior of the flow around the disk pig

downstream pipe, velocity is higher than the surrounding environment.

Figure 11 shows the obtained velocities for different diameters of bypass pig after simulation. In the initial analysis of these diagrams, the dependency of the pig velocity on the bypass diameter is fully specified. When the bypass diameter is small due to the decrease in the flow rate the pig moves with a moderate velocity close to the flow velocity in pipe. When this diameter increases the effect of environmental conditions, including the slope of the pipe, the weight and the pressure drop coefficient increases leading to significantly reduce or increase the speed of the pig in the pipeline path.

As can be seen in Fig. 11, with increasing bypass diameter, the average velocity of the pig in the pipeline decreases, on the other hand, due to the slope of the path, its speed is affected. It is seen from Fig. 11 that the mean pig velocity at $d = 1''$ is 1.22 m/s with increasing of the bypass pig diameter to $d = 5''$ the mean pig velocity decreases 34% and reaches to 0.8 m/s. Also it is seen that with increasing of the bypass pig diameter to $d = 8''$ the effect of environmental conditions, including the slope of the pipe, the weight

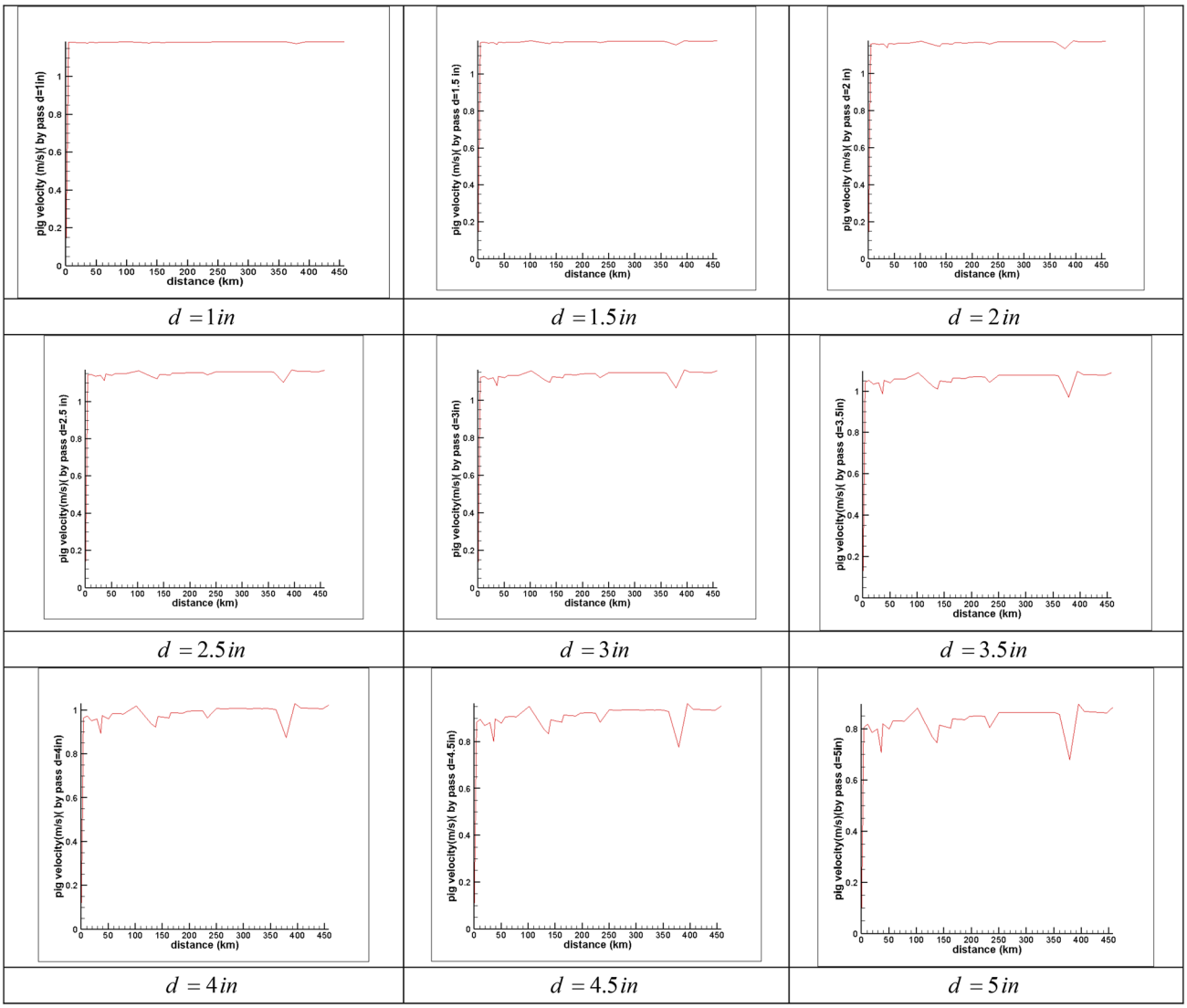

Fig. 11 The variation of pig velocity in the pipeline between Rafsanjan, Yazd and Nain with different bypass diameters

and the pressure drop coefficient increases and the mean pig velocity decreases 59% and reaches to 0.5 m/s.The effect of the slope of the pipe for uphill and downhill in the path is clears. It can be seen that the pig velocity decreases and increases with sharp slop at the path for 40–45 km, 100–145 km and 350–380 km. It is noticeable that the control of the pig velocity at these sections are important, somehow the pig velocity does not increase and decrease from authorized range. Figure 12 shows that up to 3.5 inches in bypass diameter, the average velocity of the pig has less variation than other diameters. In a 3.5 to 5 in bypass diameter, the average velocity is much lower than the previous one, and then the slope of average velocity is decreases.

With respect to the comparison of the diagrams, it is recommended that the bypass diameter of the pig does not increase by 5.5 ins, since behavior in this case is on the boundary of behavior A. Given that the recommended speed ranges 0.6 m/s to 1 m/s for pigging operations, therefore, the resulting velocity diagrams indicated that the best selected bypass diameter for this case study is equal to $d = 5$ in.

Study of dimensionless parameters affecting on flow behavior

The variation of the pressure loss coefficient according to the dimensionless groups for the different behaviors of the flow around the pig is shown in Fig. 13a–c.

Figure 13a shows a change in the horizontal bypass area $\left(\frac{d}{D}\right)^2$ in terms of the pressure loss coefficient (K_p). As shown in this figure, the flow behavior A occurs when this dimensionless group is relatively small and the flow behavior B

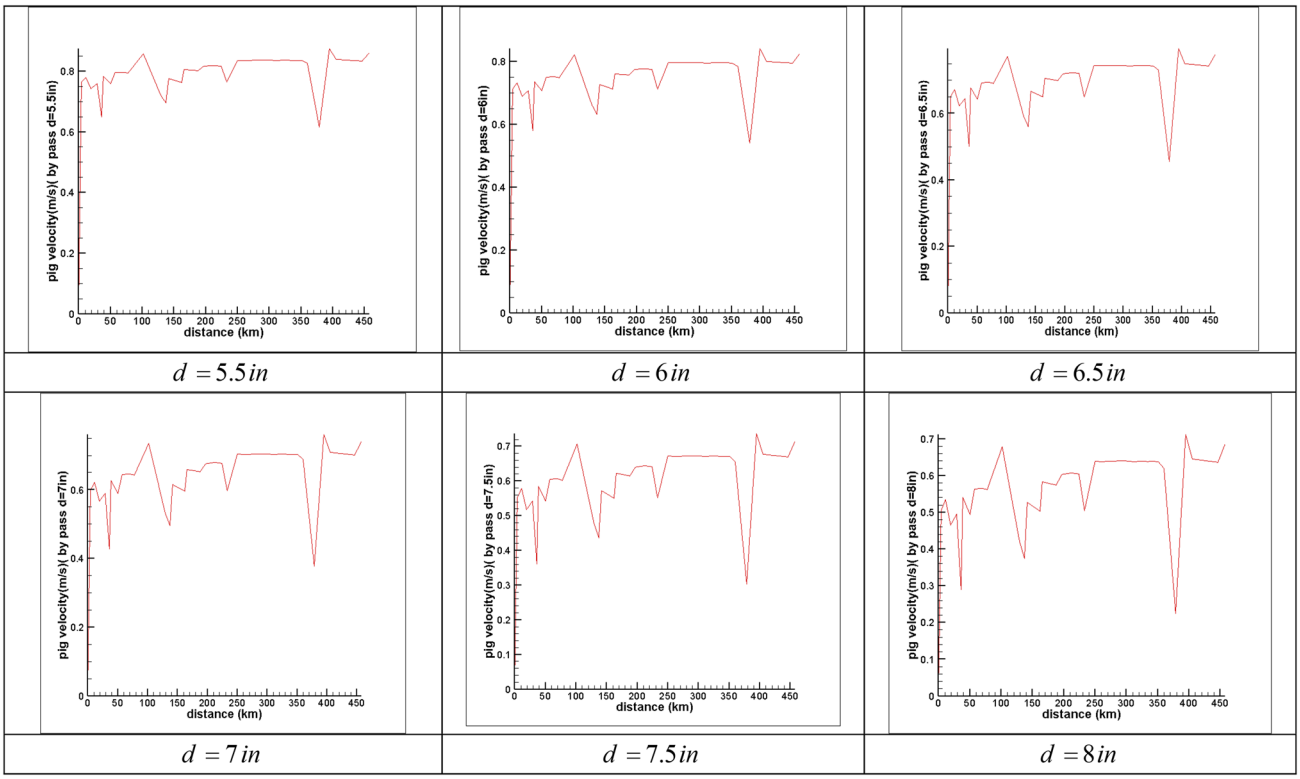

Fig. 11 (continued)

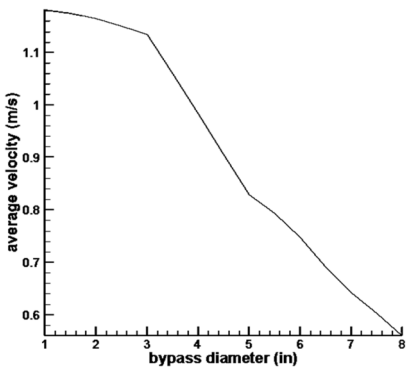

Fig. 12 Average velocity of the pig with different bypass diameters

occurs when this parameter is relatively large. Therefore, it can be concluded that if $\left(\frac{d}{D}\right)^2 < 0.0625$, then flow behavior is type A, and if $\left(\frac{d}{D}\right)^2 > 0.0625$, then flow behavior is type B.

Figure 13b shows the ratio of the diameter of the deflector plate to the disk diameter in terms of the pressure loss coefficient. As shown in this figure, if the deflector plate has a relatively small diameter, the flow behaves like B, and when the deflector plate has a relatively large diameter, the flow behaves like A. So if $\frac{H}{D} < 0.35$, the flow behavior is then type A, and if $\frac{H}{D} > 0.375$, then flow behavior is type B. In addition, Fig. 13c shows the ratio of the area of the fluid outlet level between the deflector plate and the disk pig to the disk surface $\left(\frac{4dh}{D^2}\right)$ in terms of the pressure loss coefficient. As shown in this figure, when the parameter h is relatively small, that is, the parameter is $\left(\frac{4dh}{D^2}\right) < 0.1$, the behavior of the flow around the disk pig is similar to flow behavior A, and when the parameter is $\left(\frac{4dh}{D^2}\right) > 0.1$, it transforms into the flow behavior B.

It is seen that there are two different flow behaviors for streaming around of a disk shape pig through CFD simulations (behavior A and the behavior of B). The occurrence of each of these behaviors around the pig depends on the parameters governing the pig geometry, in general, by increasing the non-dimension groups, the flow around of the pig changes from behavior A to B. It can be obtained from the simulation results to change the behavior from A to B three different options are possible, increasing of the area of the bypass path $(d/D)^2$ by increasing the bypass diameter, reducing the disk diameter in the H/D parameter along with increasing the area of fluid outlet (with increasing in the distance between the body of pig and the deflector plate, i.e., h).

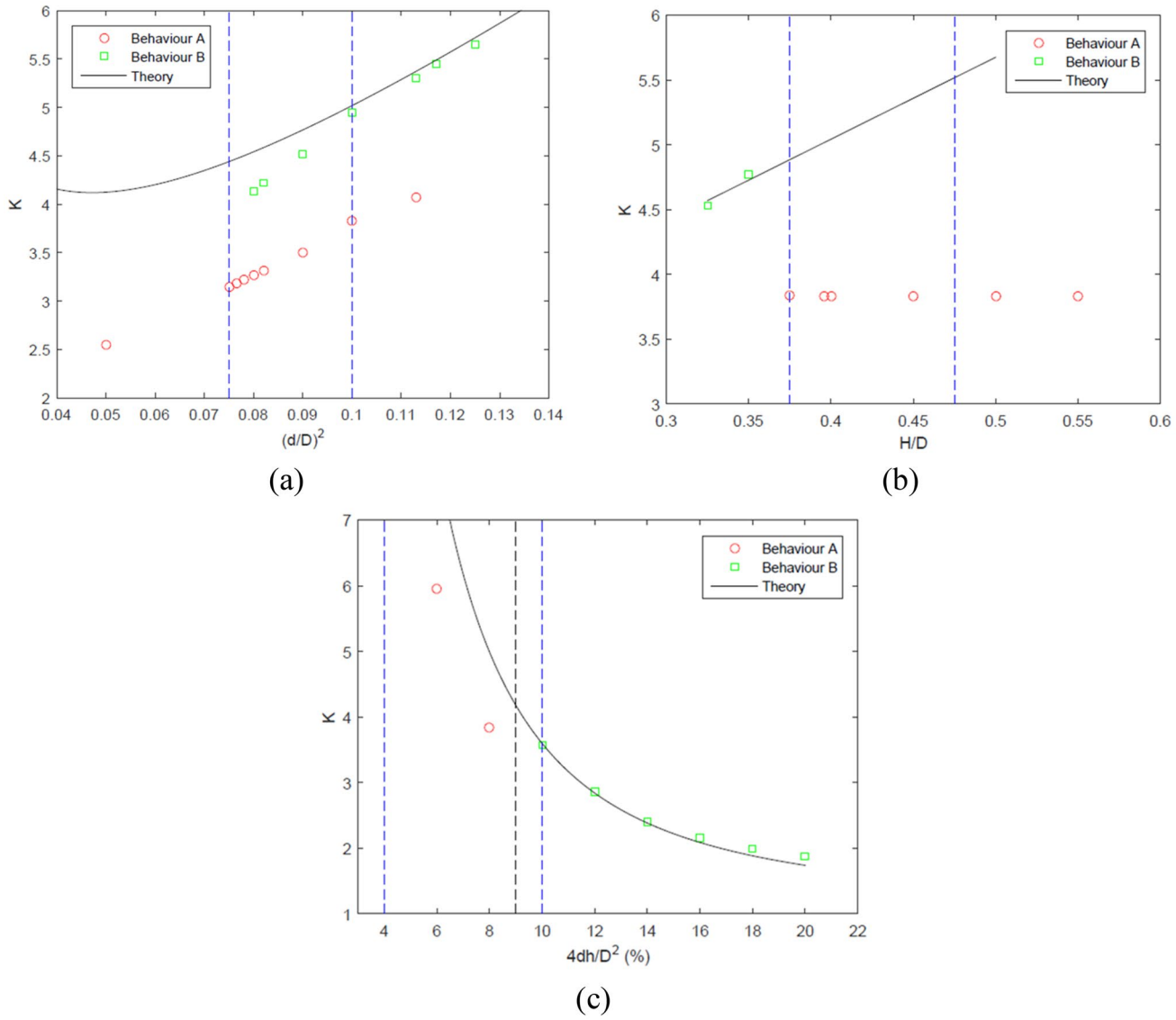

Fig. 13 The variation of pressure loss coefficient according to the dimensionless groups for the various behaviors of the flow around the considered pig

Taking into consideration the conditions above the best option of the geometric parameters size of a pig bypass with the deflector plate is when it has the lowest pressure drop, i.e., if only the lowest pressure loss in the fluid passage of the bypass is important, behavior A is very appropriate. However, it should be noted that the best cleaning mode, according to Fig. 10, occurs when behavior of flow is similar to behavior B.

So, according to the above-mentioned materials, it is found that the optimal aspect of the pig dimensions is a state which the geometric parameters of pig are determined in such a way that the flow behavior is at the end of behavior A and is transforming into behavior B. Thus, the optimal dimensions of the pig can be obtained as $\left(\frac{d}{D}\right)^2 = 0.0625$ & $\left(\frac{H}{D}\right) = 0.375$ & $4dh/D^2 = 0.1$ with respect to the values of the dimensionless groups.

A pig locator was used to carry out this experiment. The device consists of two parts. The first part is mounted on the pig body and is responsible for transmitting radio waves. The second part is the receiver of the signal, which received signals by a cord during the pig passage. Figure 14a–b shows the parts of signal transmitter and wave receiver of this device.

Fig. 14 A pig locator **a** signal transmitter **b** wave receiver

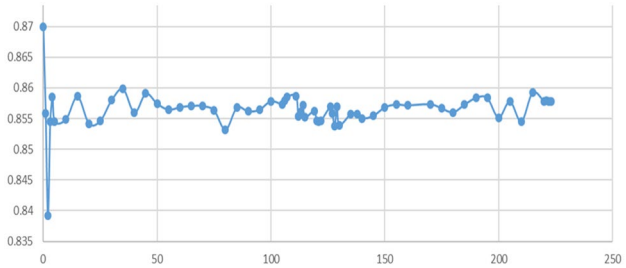

Fig. 15 The results of pig velocity (m/s) at the field test of 20 in pipeline with a disk pig and 5 inch bypass diameter

In order to conduct field test, two pig receivers were used that placed at intervals of 500 meters so that after getting the signal by the first receiver and registering the time, this receiver can pinpoint its position after the second receiver. Figure 15 shows pig velocity using the time and position of the pig. The bypass diameter in the transmitted pig is 5 inches and its specifications are in accordance with Table 1. Data from this field test are presented in Appendix 3.

By comparing the results of field test and simulation, we found an error of 4%. The study found that the following factors contributed to this difference:

1. Rubbing the pig tires due to the path length.
2. Failure to control the operator to hold constant the inlet flow rate and outlet pressure.
3. Error caused by manpower in measurement.

Conclusions

In order to control the pig velocity in the pipeline between Rafsanjan, Yazd and Nain as a case study in Iran, the desired problem as numerically is simulated hydrodynamically. According to the path map, the length of the path with respect to the pipelines included within the profile is divided into 34 cross sections according to the slope of the pipeline and its continuity, which the results of this analysis have been presented in the section below.

During the study, we found that two different flow behaviors depended on the dimensions of the bypass diameter, the distance and diameter size of the deflector plate, and the flow behavior around the pig always depended on the pig geometry. In general, the flow behavior around the pig would change from A to B if the bypass diameter increased and a similar effect is observed if the diameter of the deflector plate or the distance between the pig and the deflector plate is decreased and increased, respectively. Two completely different behaviors of A and B described around this type of pig indicated that the pressure drop across the disk pig is considered as the driving force for its motion which is strongly influenced by the flow behavior around it. It has been shown that the flow behavior B can be led to an increase of more than 30% of the pressure drop compared to the flow behavior A. The biggest difference between the two flow behavior can be the shape of the jet, which is affected by the rotating area between the pig body and the jet itself, and in both cases, the maximum velocity can occur when the jet strike the top of the disk.

Other results from this study were the total pressure drop that is considered as one of the most important measure.

1. It was found that the total pressure drop would be increased by changing the flow behavior from A to B. So, it is concluded that the driving force of pig (which is equal to the total pressure drop of the disk pig) strongly depended on the flow behavior around it.
2. In the study of the pressure difference in two sides of pig, we found that the total pressure loss occurred mainly in the bypass area and in the contact with the deflector plate.
3. For behavior A, the minimum total pressure was in the rotating area between the jet and the disk body.
4. For the flow behavior B, there is the minimum total pressure was in the rotating area between the center of the disk body and the pipe wall.
5. In the rotating areas, the static pressure was less than the surrounding. In addition, the velocity in the rotating areas was relatively low leading to a slight dynamic pressure, and therefore in the rotating area, the total pressure was lower than its surrounding area, and the center of the main rotating area had a relatively low total pressure.
6. It is found that the optimal aspect of the pig dimensions was a state that geometric parameters of pig were determined in such a way that the flow behavior was at the end of behavior A and was transforming into the behavior B. Thus, the optimal dimensions of the pig could be obtained as $\left(\frac{d}{D}\right)^2 = 0.0625 \& \left(\frac{H}{D}\right) = 0.375 \& 4dh/D^2 = 0.1$ with respect to the values of the dimensionless groups.

Appendixes

Appendix 1: profile map of the 20-in pipeline between Rafsanjan, Yazd and Nain

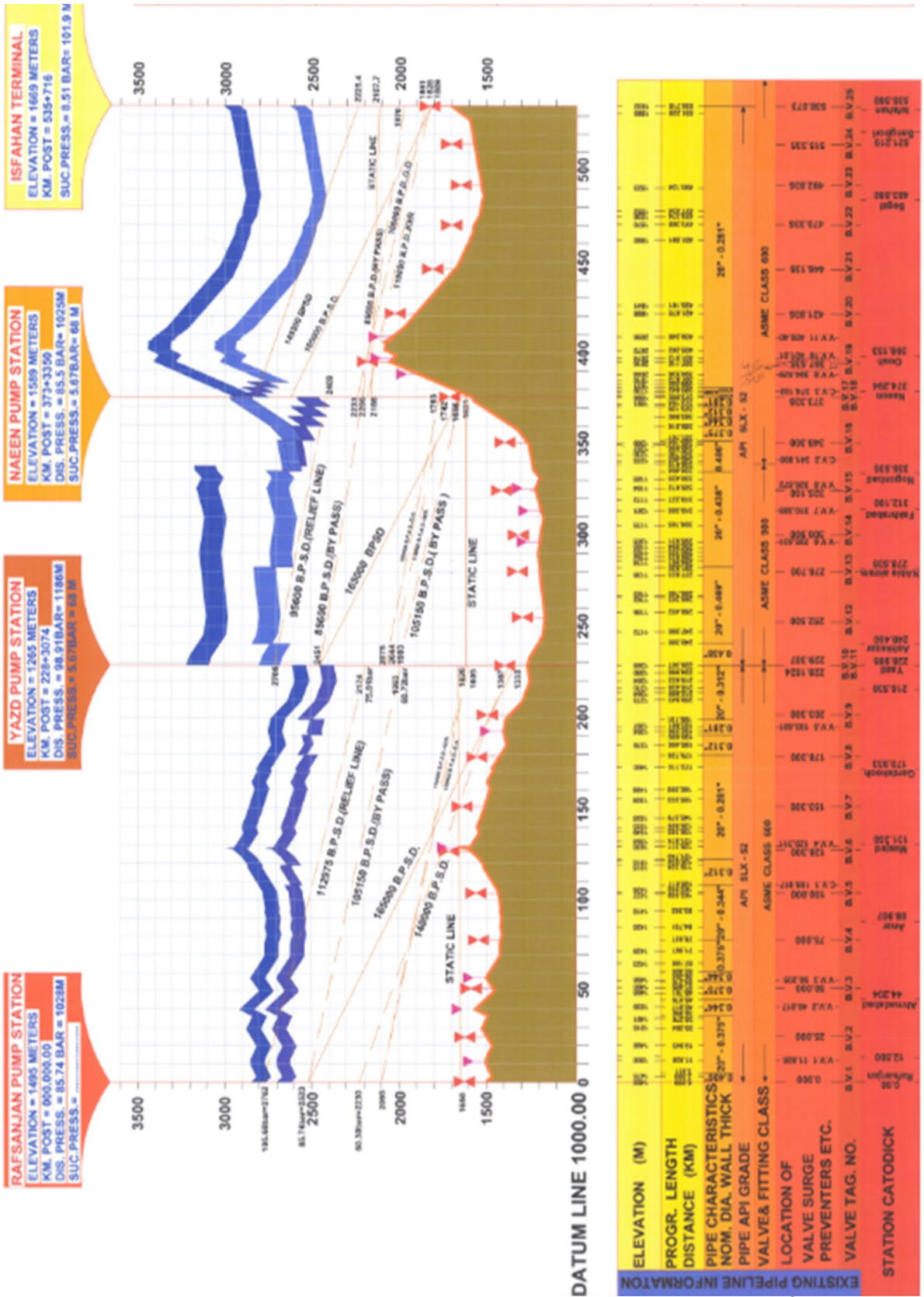

Appendix 2: specifications associated with different parts of the desired pipeline

Static pressure at the end-point of section (Pa)	Gravity in x-direction (m/s^2)	Gravity in y-directin (m/s^2)	Sin of angle of section (°)	Angle of section (°)	Length of section (m)	Elevation in start-point of section (m)	No. of section
12,452.97	0.1	9.81	0.01	0.00823	7	1452.53	1
11,768.2	−0.1	9.81	−0.01	−0.01032	8	1511.21	2
13,029.56	0.2	9.81	0.02	0.016668	10	1428.11	3
12,637.07	−0.1	9.81	−0.01	−0.00662	7	1581.18	4
14,095.45	0.49	9.81	0.05	0.047927	3	1533.55	5
11,657.78	−0.29	9.81	−0.03	−0.02878	11	1710.53	6
12,628	0.2	9.81	0.02	0.016591	7	1414.71	7
10,773.09	−0.2	9.81	−0.02	−0.01707	13	1532.45	8
10574.91	0	9.81	0	−0.003	8	1307.35	9
10,759	0	9.81	0	0.000915	24	1283.3	10
14,835.27	0.2	9.81	0.02	0.018535	27	1305.64	11
13,469.18	−0.2	9.81	−0.02	−0.02047	8	1800.31	12
13,759.16	0.1	9.81	0.01	0.007625	5	1634.53	13
11,998.43	−0.1	9.81	−0.01	−0.0105	20	1669.72	14
12,483.3	0.1	9.81	0.01	0.014077	4	1456.05	15
9748.72	−0.2	9.81	−0.02	−0.01531	22	1514.89	16
10,036.72	0	9.81	0	0.003778	9	1183.04	17
7694.57	−0.2	9.81	−0.02	−0.01962	15	1217.99	18
6618.84	−0.1	9.81	−0.01	−0.011	12	933.762	19
6907	0	9.81	0	0.003961	9	803.218	20
4855.77	−0.1	9.81	−0.01	−0.01465	17	838.187	21
4754.24	0	9.81	0	−0.00127	9	589.264	22
5420.07	0	9.81	0	0.002259	36	576.943	23
4732.01	−0.1	9.81	−0.01	−0.00534	16	657.743	24
5795.17	0.1	9.81	0.01	0.0075	17	574.245	25
5305.79	−0.1	9.81	−0.01	−0.00935	6	703.263	26
6082.79	0.29	9.81	0.03	0.025219	4	643.875	27
6660.94	0.1	9.81	0.01	0.005219	13	738.167	28
8019.74	0.2	9.81	0.02	0.018834	9	808.327	29
15,214	0.49	9.81	0.05	0.047266	19	973.222	30
24,939.74	0.69	9.81	0.07	0.0729	16	1846.27	31
25,519.2	0.1	9.81	0.01	0.0067	10	3026.52	32
15,865.98	−0.29	9.81	−0.03	−0.0285	41	3096.84	33
14,498.41	−0.1	9.81	−0.01	−0.01447	12	1925.39	34

Appendix 3: the time of pig passage in different km of pipeline from Rafsanjan to Yazd in the field test

Km of pig passing in pipe line	Date	Time
1	4-May	13:22:34
4	4-May	14:03:22
11	4-May	16:00:29
19	4-May	19:11:31
29	4-May	23:04:19
36	5-May	1:41:46
39	5-May	2:35:02
50	5-May	6:03:22
57	5-May	8:05:46
70	5-May	13:33:07
78	5-May	15:47:02
102	6-May	0:13:26
129	6-May	9:33:36
137	6-May	11:42:43
142	6-May	13:35:02
162	6-May	20:21:36
166	6-May	22:54:43
188	7-May	5:52:19
197	7-May	8:08:10
212	7-May	13:49:55

References

Azevedo LFA, Braga AMB, Nieckele AO (1996) Simple hydrodynamic models for the prediction of pig motions in pipelines. Offshore Technol Conf Ann Proc 4:729–739

Braga AMB, Azevedo LFA, Nieckele AO, Souza Mendes PR (1998) Pipeline pigging simulation project, final report, department of mechanical engineering, PUC-Rio, Brazil

Davodian M (2014) Modeling of pigs in oil and gas pipe lines, Master's thesis, Shahid Bahonar University, Iran (In Persian)

Esmaeilzadeh F, Mowla D, Asemani M (2009) Mathematical modeling and simulation of pigging operation in gas and liquid pipelines. J Petrol Sci Eng 69:100–106

Hosseinalipour SM, ZarifKhalili A, Salimi A (2007) Numerical simulation of pig motion through gas pipelines. In: 16th australasian fluid mechanics conference, Australia, pp. 971–975

Idelchik IE (1987) Handbook of hydraulic resistance, 2nd edn. Hemisphere Publishing Corporation, Washington

Kohda K, Suzukawa Y, Furukwa H (1988) A new method for analyzing transient flow after pigging scores well. Oil Gas J 9:40–47

Korban JEA (2014) CFD modeling of bypass pigs, Master's thesis, Delft University of Technology, Netherlands

Lesani M, Rafeeyan M, Sohankar A (2012) Dynamic analysis of small pig through two and three dimensional liquid pipeline. J Appl Fluid Mech 5(2):75–83

McDonald A, Baker O (1964) Multiphase flow in (Gas) pipelines. Oil Gas J 62(26):64–67

Nguyen TT, Kim SB, Yoo HR, Rho YW (2001) Modeling and simulation for pig flow control in natural gas pipeline. J Mech Sci Technol 15(8):1165–1173

Nshuti RF (2016) Dynamic analysis and numerical simulation of PIG motion in pipeline, Master's thesis, Chonnam National University, South Korea

Ramirez R, Dutra M (2011) Evaluating drag force and geometric optimisation of pipeline inspection gadget (PIG) body with bypass. Ingeniería E. Nvestigación 31(2):152–159

Saeedbakhsh M, Rafeeyan M, Sohankar A (2009) Dynamic analysis of small pigs in space pipelines. Oil Gas Sci Technol 64(2):155–164

Singh A, Henkes RAWM (2012) CFD modelling of the flow around a by-pass pig. In: 8th North american conference on multiphase technology, 229